ADVANCED MATERIALS

DOI: 10.1002/adma.200502566

A Two-Dimensional $KTiOPO_4$ Photonic Crystal Grown Using a Macroporous Silicon Template**

By *Alexandra Peña*, *Sergio Di Finizio*,* *Trifon Trifonov*, *Joan J. Carvajal*, *Magdalena Aguiló*, *Josep Pallarès*, *Angel Rodriguez*, *Ramón Alcubilla*, *Luis F. Marsal*, *Francisco Díaz*, and *Jordi Martorell**

Photonic crystals (PCs) are an ideal framework to control optical nonlinear interactions. Since 1995, it has been shown that within a PC one may enhance,[1–3] phase match,[4,5] or hold a non-vanishing second-order interaction even if the material is centrosymmetric.[6] More recently, it has been pointed out that the structuring of the dielectric together with modulation of the second-order nonlinear susceptibility may lead to a backward parametric oscillation,[7] a nonlinear effect predicted many years ago that has not yet been observed. All such control over the nonlinear interaction is possible in 1D, 2D, or 3D PCs. Among them, 2D photonic structures are, perhaps, the most interesting, because such structures could, in principle, be easier to integrate into optoelectronic devices meant for light amplification, light generation at other frequencies, optical-data processing, or any kind of sensing.[8–11] The fabrication of 2D PCs using top-down procedures such as electron-beam lithography has been applied successfully in several kinds of semiconductors.[12–14] Unfortunately, patterning of inorganic crystals applying, for instance, focused-ion-beam bombardment and subsequent reactive-ion etching is limited to small depth/diameter ratios.[15] Developing procedures that would be more efficient in patterning inorganic crystals is very interesting for the fabrication of new light modulators that could take full advantage of the nonlinear optic and electro-optic coefficients of such materials.[16] On the other hand, neither the viability nor cost-effectiveness of integrating some very expensive nonlinear semiconductors in silicon-based devices have been clearly demonstrated. There are alternative routes to pattern inorganic nonlinear optical materials, such as $KTiOPO_4$ (KTP) or $LiNbO_3$ routes based on a periodical poling followed by a selective domain etching.[17] Although periodical poling has been applied with different degrees of success to obtain 1D arrays with a sub-micrometer period in some nonlinear materials,[18] it is still difficult to accurately control the size of small domains. Moreover, after poling one ends up with a stand-alone sample that would, certainly, be difficult to embed in any silicon-based device. We present here a completely novel combination of both top-down and bottom-up approaches to grow 2D PCs of KTP. These crystals are grown in ordered macroporous silicon templates. An additional benefit of such an approach is that, while being simple, the silicon matrix and the structured nonlinear material, which would eventually be used to modulate or generate light, forms an integral unit. To fabricate such a hybrid structure, an ordered silicon matrix of air holes and a KTP substrate were kept closely bound in a growth solution of KTP. We observed that KTP columns grew inside the air holes of the silicon matrix following the crystalline orientation of the substrate. Finally, the potential of the 2D array of KTP columns to control the nonlinear interaction was demonstrated by measurement of the diffraction pattern at the second harmonic (SH) frequency of the incident light. Such a pattern was obtained using a sample where the KTP columns had been polished down to an optical-quality surface and where the silicon template had been partially etched.

The 2D KTP patterning we implemented may be summarized in a four-step procedure that involves the preparation of a high-quality ordered macroporous silicon template, the growth of KTP columns into the silicon template, the polishing of the top or bottom surface of the KTP columns, and finally a partial selective etching of the silicon matrix. The sequence of these four steps is shown schematically in Figure 1. There are several reasons that make macroporous silicon an excellent matrix for growing 2D PCs of KTP. On one hand, it has been shown that one may fabricate 2D silicon structures with a wide range of lattice parameters that may be as small

[*] S. Di Finizio, Prof. J. Martorell
ICFO-Institut de Ciències Fotòniques
Mediterranean Technology Park
08860 Castelldefels, Barcelona (Spain)
E-mail: sergio.di.finizio@icfo.es; jordi.martorell@icfo.es
Prof. J. Martorell
Departament de Física i Enginyeria Nuclear
Universitat Politècnica de Catalunya
C/Colom, 11, 08222 Terrassa, Barcelona (Spain)
A. Peña, Dr. J. J. Carvajal, Dr. M. Aguiló, Prof. F. Díaz
Física i Cristallografia de Materials (FiCMA)
Universitat Rovira i Virgili
Campus Sescelades
c/Marcel·lí Domingo, s/n, 43007 Tarragona (Spain)
Dr. T. Trifonov, Prof. J. Pallarès, Prof. L. F. Marsal
Departament d'Enginyeria Electrònica, ETSE
Universitat Rovira i Virgili
Avda. Països Catalans 26, 43007 Tarragona (Spain)
Prof. A. Rodriguez, Prof. R. Alcubilla
Departament d'Enginyeria Electrònica
Universitat Politècnica de Catalunya, C4-Campus Nord
Jordi Girona, 1–3, 08034 Barcelona (Spain)

[**] We acknowledge Dr. Josep Ferre-Borull for help in performing the FTIR measurements; the Ministerio de Educación y Ciencia, for supporting the work (Grant Nos. MAT2002-04603, TIC2002-04184, MAT2005-06354, and TEC2005-02038). We also acknowledge support from the EC-funded project PHOREMOST (FP6/2003/IST/2511616) and J. M. acknowledges support from the Generalitat de Catalunya that funded the work with the "Distinció de La Generalitat de Catalunya per a la promoció de la recerca universitària."

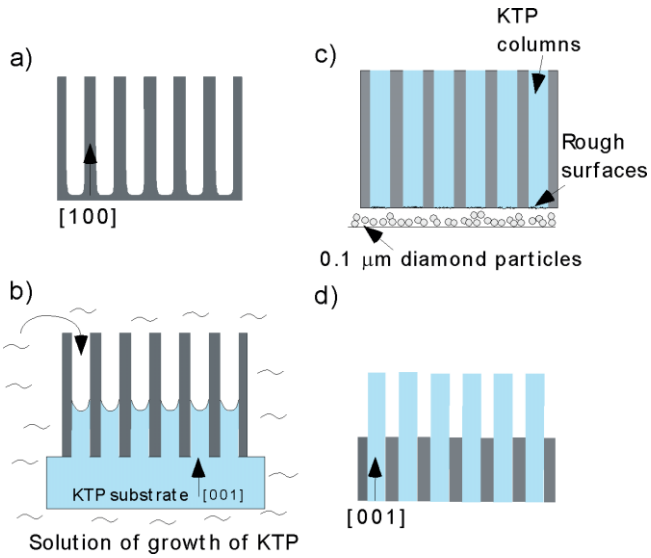

Figure 1. Schematic view of the four stages of growth of KTP 2D PCs: a) preparation of the oriented 2D macroporous silicon membrane, b) the silicon template is attached to an oriented KTP substrate and then immersed in the growth solution of KTP. The direction of column growth is the same as the KTP crystallographic direction, [001]. c) After growth, the top of the columns is polished with diamond particles in order to obtain an optical-quality surface. d) Silicon is partially removed by selective chemical etching.

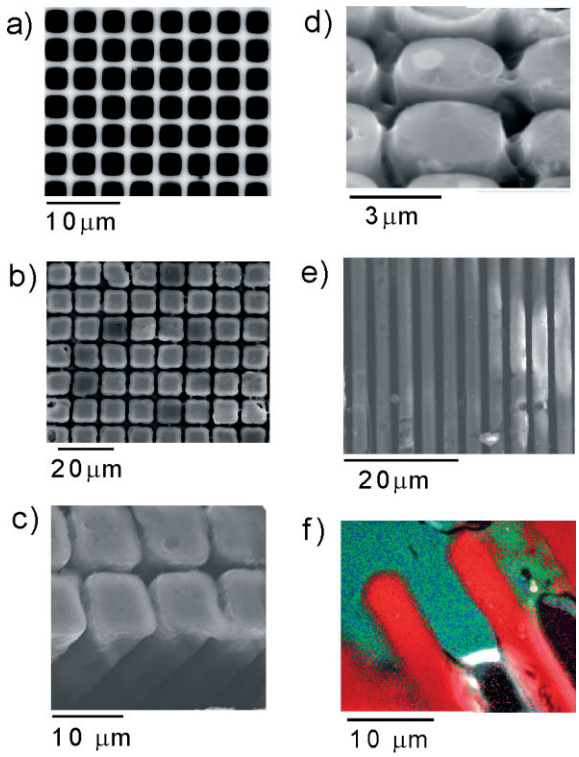

Figure 2. Scanning electron microscopy (SEM) images: a) a macroporous silicon 2D square lattice membrane, b) top surface of a 2D KTP PC after polishing and partial etching of the silicon mask, and c) side view of the 2D KTP PC where one clearly sees that the silicon template has been selectively etched from the KTP. d) Detailed view of a 2D KTP crystal with a period of 4.5 μm, which was also used for the optical measurements. e) Side view of a plane of columns of a 2D KTP PC lattice. f) Energy-dispersive X-ray analysis of the KTP columns grown within the air holes of the silicon matrix: red dots indicate the presence of silicon, green dots indicate potassium, and blue dots indicate titanium. Images (b,c,e) were taken without the deposition of a gold layer so the samples could be used for later optical measurements.

as 0.5 μm[19] and have pore depths exceeding 200 μm. On the other hand, the melting temperature of silicon is 1687 K, 414 K higher than the growth temperature of KTP. We prepared the silicon membranes by light-assisted electrochemical etching[20] and post-processing. The starting material was n-type <100> silicon with a resistivity of 2–6 Ω cm. The front side of the wafers was patterned with inverted pyramid-shaped pits by oxidation, photolithography, and subsequent tetramethyl ammonium hydroxide (TMAH) etching. The pattern consisted of inverted pyramids with a square base arranged in a square periodic lattice. We patterned different samples with pyramid bases that ranged from 2 μm × 2 μm to 8.5 μm × 8.5 μm, while the period of the lattice ranged from 4.5 to 10 μm. These inverted pyramids act as nucleation sites for the ordered pore growth. On the back side of the silicon wafer an indium tin oxide (ITO) film was sputtered to provide a low-resistance transparent ohmic contact. The wafers (as working electrode) were incorporated in an electrochemical etching cell containing a 2.5 wt % aqueous solution of HF acid. The chemical dissolution of the silicon requires the generation of positive carriers (holes), which is achieved using a 100 W halogen lamp for back-side illumination. The quality and size of the pores was controlled by a computerized feedback mechanism that regulated the generation of holes by continuously adjusting the back-side illumination to maintain a constant current. After pore growth, the ITO layer was removed and the back side of the wafer polished down until the holes opened, thereby obtaining a free-standing silicon template. As shown in Figure 2a, the pores of the silicon templates were very uniform in size.

In a second step, a platinum wire was used to bind the silicon template to a single KTP crystal with dimensions that were usually 5 mm long by 3.5 mm wide by 1 mm thick. The crystal was oriented so the largest surface was perpendicular to the *c* crystallographic direction with the edges parallel to the *a* and *b* crystallographic directions. The *c* crystallographic direction of these KTP plates was extremely accurately determined from an X-ray texture characterization during the lapping and polishing processes. The template/substrate was dipped for 5 min into the high-temperature solution, where a degree of supersaturation of about 2 % had been created, without any additional thermal gradient. Then, the template/substrate/epitaxy composite was removed from the solution, but kept inside the furnace above the surface of the solution while the furnace was cooled to room temperature at a cooling rate of 15 K h^{-1} to avoid thermal stresses that could result in cracks, either in the 2D photonic structures or in the substrate.

After growth, the top part of the KTP columns formed an irregularly shaped meniscus that, for many applications, must

ADVANCED MATERIALS

be removed. In principle, it was possible to flatten the top of the columns by mechanically polishing the sample. However, the hardness of silicon is seven on Mohs scale, significantly higher than that of KTP, which is only approximately 4.5. As a consequence, it was not easy to polish both materials at the same time to obtain columns with an optical-quality top surface. After several attempts, following different procedures, a good result was obtained using diamond powders with a particle size of 0.1 μm. In Figure 2b one sees the top part of the polished, square-shaped columns of KTP embedded in the silicon template. Once an optical-quality surface for the KTP columns was obtained, the last step was to remove the silicon template by selective chemical etching with TMAH diluted in distilled water (5 vol %) at 354 K. The etching rate of the <100> face was 1.4 μm min^{-1}. The effect of the selective etching is clearly visible in Figure 2c, where a scanning electron microscopy (SEM) side-view image of the KTP columns is shown. From this image, it is clear that the final 2D PC is formed of independent KTP columns.

We fabricated samples with lattice parameters ranging from 4.5 to 10 μm (see Fig. 2d). In the data we collected from the growth procedure we followed there is nothing to indicate that 2D KTP PC with smaller diameter columns could not be grown, as macroporous silicon templates with a smaller diameter pore are readily available. In the space where the silicon was etched, there are some bridges of material connecting adjacent columns, visible in Figure 2b–d. These bridges are probably the remains of TMAH, which was very viscous and difficult to remove.

To obtain a side view of the columns, we polished the sample at a small angle with respect to the axis of the columns. Then, a length of 35 μm of the side of the columns was visible in between one plane and the next, as shown in Figure 2e. In that figure, the aspect ratio (height/diameter) is 14:1. On average, when using a 100 μm silicon template and after the full process to obtain optical-quality samples was completed, we estimated that the length of the columns was 70–80 μm, resulting in an aspect ratio in the range 28–32.

The chemical composition of the columns was measured using energy-dispersive X-ray analysis, shown in Figure 2f, from which we concluded that the columns were formed exclusively of KTP. In Figure 2f, one clearly sees that the KTP columns grow from the substrate, whereas the silicon mask acts as a template for the growth. The columns of silicon, in red, most probably correspond to the thicker part of the template located at the intersection points of the lattice. In the samples used for X-ray or optical measurements, we also polished the other side of the sample to remove the KTP substrate to ensure that only the 2D ordered structure of KTP and silicon remains. Using this method, the results obtained from the structural and optical characterizations will be from the 2D ordered structure only. The final 2D PCs are formed from square columns of KTP surrounded by air on the higher part of the columns and by silicon on the lower part. The silicon in the lower part is maintained to give the sample the necessary mechanical rigidity.

To compare the crystallographic orientation of the 2D photonic structure of KTP with respect to the crystallographic orientation of the original KTP substrate used as a seed for column growth, we performed an X-ray texture analysis of the final 2D columnar structure. This procedure also provides an estimation of the degree of crystallinity of the columnar structure. The orientation of the pillars relative to the crystallographic axes is shown in Figure 3a, while Figure 3b shows the 2θ scan for the KTP PC (pattern i) and the substrate (pattern ii). As can be seen, the peak with the highest intensity in these patterns is the (004) peak. The full width at half maximum (FWHM) for the (004) peak in the photonic structure was found to be 0.4°, very similar to that of the initial substrate. This shows the high degree of crystallinity of the photonic structure. The inset in Figure 3b shows the (004) and (204) pole figures corresponding to the 2D KTP columnar structure. These pole figures confirm the high degree of orientation of the axis of the KTP columns parallel to the *c* crystallographic direction, and at the same time give information about the location of the *a* and *b* crystallographic directions (parallel to the edges of the substrate). The X-ray powder dif-

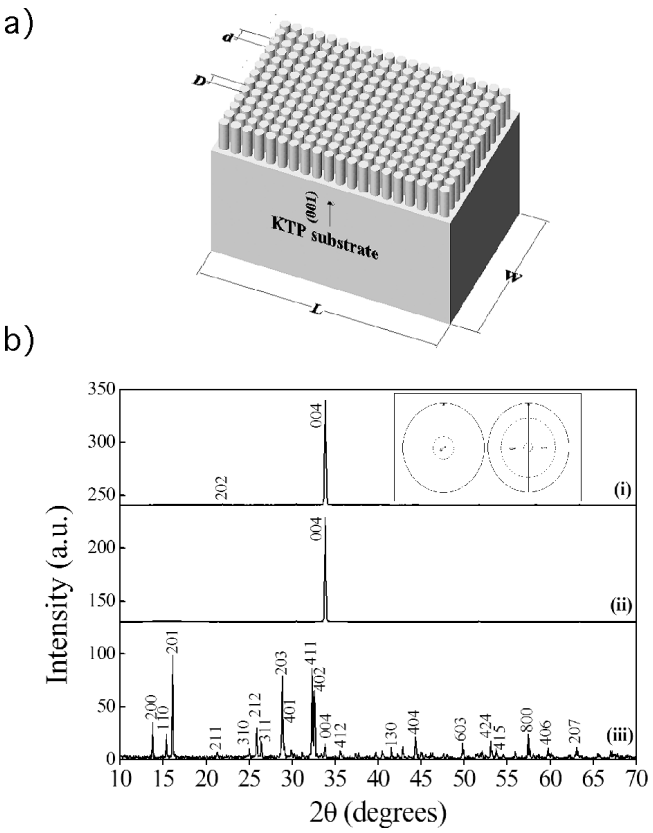

Figure 3. a) Schematic view of the KTP columns on top of the KTP substrate showing the crystallographic direction, where *L* is parallel to the crystalographic direction *a* and *W* is parallel to the crystalographic direction *b*. b) X-ray texture analysis: i) 2θ scan for the photonic structure, ii) 2θ scan for the substrate, and iii) 2θ scan for KTP crystalline powders; inset: (004) and (204) pole figures corresponding to the 2D KTP PC.

fraction pattern obtained for a KTP crystalline powder sample, milled from a single crystal, is also shown in Figure 3b (pattern iii) to compare the degree of texturization of the columnar sample. The reflections were indexed according to the powder diffraction pattern of KTP, entry 80-0893 of the database maintained by the Joint Committee for Powder Diffraction Studies (JCPDS).[21] We observe that the peak with the maximum intensity in the powder diffraction pattern is not the one corresponding to the (004) plane, which indicates, again, the high degree of texturization and orientation of the KTP columns grown from the KTP substrate.

To demonstrate the PC properties of the 2D structures grown, we performed a measurement of the specular reflection as a function of the wavelength of the incident field, which is shown in Figure 4a. A dip in this reflection spectrum should be found when the wavevector component of the transmitted field, which lies on the plane that separates the top of the KTP columns from air, couples to any one of the forbidden bands of the 2D band structure.[22] The 2D PC we used was a square lattice of KTP columns in air with a 4.5 μm periodicity in the ΓX direction. In that sample where the top of the columns had been polished to an optical quality surface, 8 to 10 μm of silicon had been partially removed after approximately six minutes of selective chemical etching. In other words, the 2D PC we measured was a KTP–air square lattice. We placed the sample on an *xyz* positioning stage mounted on a rotating stage to set the angle of incidence, as shown schematically in Figure 4b. Using the *xyz* positioning stage and with the help of a charge-coupled device camera, the sample was placed close to the focal point of a 10 cm lens used to focus the laser-light pulses. An optical parametric amplifier pumped by the SH of linearly polarized 1 ps laser pulses at 1055 nm was used as the tunable laser source. The light was incident on the top of the columns at a fixed angle of 25° with respect to the axes of the columns. The wavelength of the incident light was tuned in the spectral range of 940–1220 nm, while the reflected light was detected using a pyroelectric detector with a flat response in that range. For the entire tuning

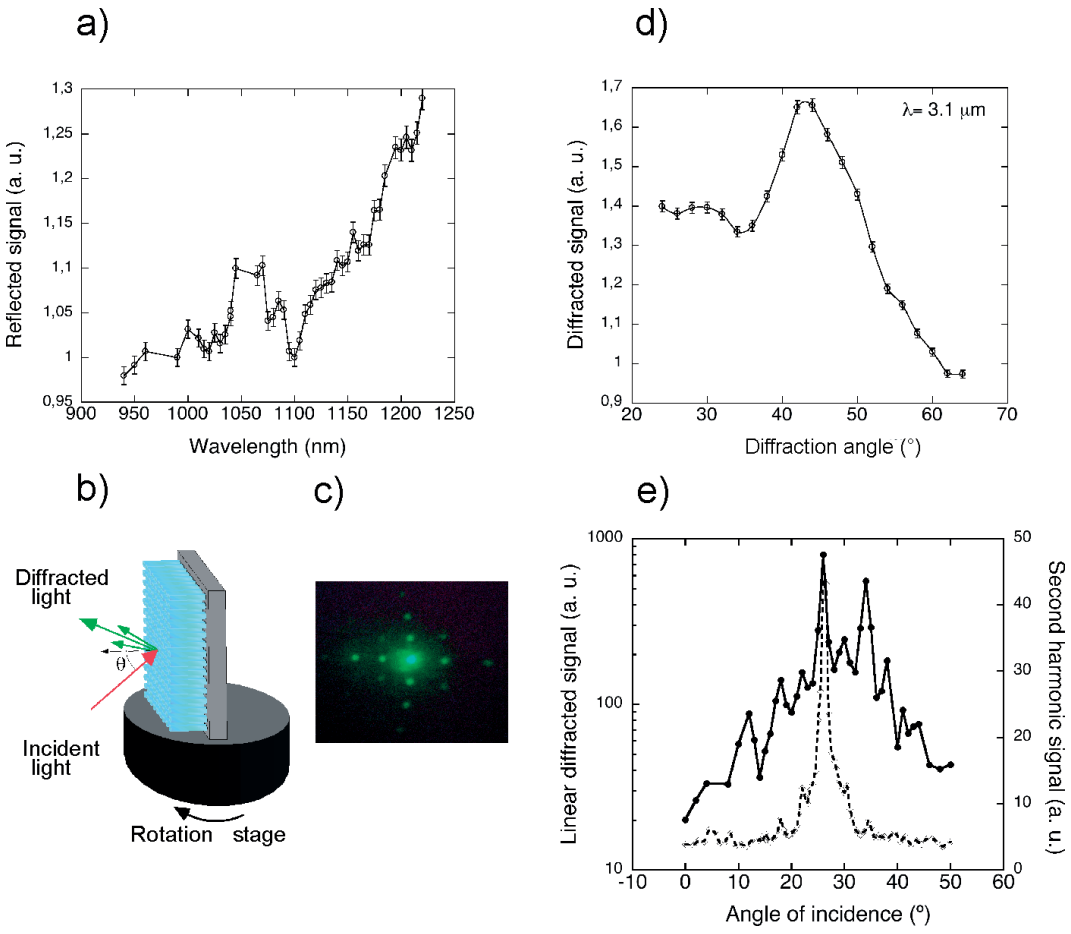

Figure 4. Photonic band, linear, and nonlinear diffraction measurements of a 2D square lattice of columns of KTP in air with a lattice parameter of 4.5 μm. a) Measurement of the specular reflection as a function of the wavelength of the incident light. The angle of incidence was set to 25°. b) Experimental setup used for the measurement of the photonic band, the linear and the nonlinear diffraction pattern. This schematic figure shows the rays for nonlinear diffraction only. c) Picture of the linear-diffraction pattern at $\lambda = 527$ nm. d) Measurement of the first linear diffracted order in reflection at $\lambda = 3.01$ μm. e) Intensity of the linear diffracted light at 527 nm in reflection as a function of the angle of incidence (empty circles) and SH intensity as a function of the angle of incidence obtained when pumping the sample with light at 1055 nm (solid dots). The lines shown in all figures are a guide for the eye.

ADVANCED MATERIALS

range the incident pulses were linearly p-polarized. As seen in Figure 4a, a dip in the specular reflectance was found when the incident light was tuned at 1100 nm. The spectral position of the dip coincides with the spectral position of the third-order Bragg reflection band that we determined from a numerical calculation of the transmission in the ΓX direction using the transfer matrix formalism.[23] In Figure 4a one also sees a decrease in the reflected intensity as the frequency of the laser increases, which may be attributed to scattering losses proportional to the fourth power of the frequency of the incident light.

The 2D pattern of KTP columns is also apparent from the diffraction of reflected light since the surface of the 2D PC of KTP acts as a 2D diffraction grating. With the sample mounted as shown in Figure 4b, it was illuminated with the SH at 527 nm of the linearly polarized 1 ps laser pulses at 1055 nm. The observed diffraction pattern is shown in Figure 4c. As expected, the pattern we observed corresponds to a 2D square lattice with a lattice parameter of 4.5 μm. We may extend such diffraction measurements in reflection to the IR (1–4 μm) range of wavelengths using a Fourier transform spectrometer (Brucker Vertex 70). The IR beam was normally incident on the sample and the diffracted light was collected for all the wavelengths within that range at several angles from 24° to 64°. Figure 4d shows a peak corresponding to the first diffracted order at 42° when the wavelength of the incident light was 3.01 μm. All three linear measurements, the photonic band, the visible-light diffraction, and near-IR light diffraction are in agreement, and correspond to a 2D square lattice of KTP columns with a lattice parameter of 4.5 μm.

We also performed some preliminary nonlinear measurements to prove the viability of the fabricated structure as a source for nonlinear generation of light. In that event, the sample was placed in the same setup described above, except that in this case the laser pulses at 1055 nm were directly incident onto the sample. The SH light generated in reflection from the KTP columns was filtered from the reflected fundamental with the use of heat-absorbing filters and an interference filter centered at 527 nm and measured using a photomultiplier tube. In Figure 4e, we observe that the generated SH as a function of the angle of incidence exhibits a clear SH peak located in the same position as the zero-order peak of the linear diffraction pattern. Peaks at other positions that would appear when the phase matching condition between the fundamental wavevector $\mathbf{k}_{\omega}$, and the SH wavevector $\mathbf{k}_{2\omega}$[24]

$$\mathbf{k}_{2\omega} = 2\mathbf{k}_{\omega} + \mathbf{G} \quad (1)$$

is satisfied for reciprocal lattice vectors G other than zero are still visible, but they appear somehow embedded in the background. One should not expect to obtain a large contrast ratio for such higher-order peaks given the weak diffraction power of the lattice at orders higher than zero order as observed in the linear pattern of diffraction shown in Figure 4e. This is a consequence of reflection measurements, which are very sensitive to the optical quality of the top surface of the KTP columns.

In conclusion, we present a completely new procedure to fabricate nonlinear 2D PCs of KTP. Such crystals are integrated in a silicon matrix that could either be removed or not in accordance to the specific application intended for the 2D structure we propose. The X-ray measurements performed to determine the crystallographic character of the grown KTP columns showed that with the procedure presented we have full control of the crystalline direction of growth with respect to the direction of the columns of the 2D structure. This is important since one may use the most appropriate nonlinear or electro-optic coefficient in combination with a phase-matching condition, which would be provided by the 2D photonic structure. This is not possible with bulk KTP where phase matching relies on the birefringence and the coefficients with the largest nonlinearity cannot be used for efficient SH generation. Finally, we have demonstrated experimentally the PC properties of the 2D structures we fabricated through measurement of the third-order forbidden band in the ΓX direction and from measurements of light diffraction in the visible and near-IR region of the spectrum. These structures may find applications in the generation of light at higher frequencies, the electro-optic modulation of light, the backward parametric amplification and oscillation, and should be very easily integrated into silicon-based devices.

Experimental

Silicon wafers were anodized in 2.5 wt % aqueous HF acid electrolyte at 293 K. An anionic surfactant, sodium dodecyl sulfate, was added to the electrolyte at a concentration of about 0.1 mM in order to reduce the surface tension and to avoid sticking of hydrogen bubbles to the wafer surface. For the same reason, the electrolyte was continuously stirred. The wafer backside was illuminated using a 100 W halogen lamp to generate positive charge carriers (holes), which are required for the chemical dissolution of silicon. To stop deep-penetrating IR light and thus, to prevent hole generation near the front-wafer surface, the lamp was coupled to a dielectric heat-reflecting mirror (SIR, Praezisions Glas & Optik) transmitting wavelengths below 750 nm. An anodic bias of 1.5 V was applied across the sample which creates a space-charge region (SCR) evolving within the silicon electrode. The generated SCR focuses the positive carriers and localizes the dissolution reaction mainly at the tips of the nucleation sites [25]. This results in the growth of straight pores along the <100> direction. The applied voltage was measured in relation to the reference electrode (platinum wire) positioned close (3 mm) to the wafer. The current density was kept at 5 mA cm^{-2} during the etching by controlling the backside-illumination intensity. The pore diameter is proportional to the number of positive charge carriers that are collected by the pore tip, which in turn depends on the intensity of the backside illumination. Keeping the etching current constant is needed to get straight pores. The pore length is determined by the duration of the HF etching process. In the experimental conditions described above, 100 μm long pores are etched in almost 4 h. This results in a mean etching rate of about 0.46 μm min^{-1}.

Liquid phase epitaxy (LPE) is the technique used in the present work to grow 2D ordered crystal structures of KTP. Given that KTP melts incongruently we used hydrothermal and flux-growth methods [26,27]. The 2D KTP photonic structures are grown using a homoepitaxial process on a KTP substrate dipped in a solution formed by the

mixing of K_2O, P_2O, TiO_2, and WO_3 with the mol % composition of $K_2O/P_2O_5/TiO_2/WO_3 = 42:14:14:30$. WO_3 is used as a modifier of the solution to decrease its viscosity and to allow the process of growth to be developed more quickly [28]. The LPE experiments were performed in a special vertical furnace built to provide a wide enough region in which there was practically no axial gradient. The temperature was controlled using a Eurotherm 903P controller programmer. 50 g of solution were prepared in platinum cylindrical crucibles 30 mm in diameter and 40 mm high. In order to establish a controlled supersaturation degree in the solution, we need a precise determination of the saturation temperature, T_s. This value was determined by varying the temperature of the solution and observing the growth or dissolution of a thick single crystal of KTP in contact with the surface of the solution. The T_s established was 1213 K. We initiated the epitaxial growth of the KTP 2D photonic structure two degrees below the saturation temperature, which provided a supersaturation in the solution of about 2 %.

The X-ray texture characterization was performed with a Siemens D5000 diffractometer equipped with an Euler goniometer to obtain the 2θ scan from 10° to 70°, with a step size (*ss*) of 0.05° and a step time (*st*) of 3 s. Using the same diffractometer equipped with a Schulz goniometer we obtained the 004 pole figure at $2\theta = 33.85°$; $\chi = 0–15°$, $ss = 3°$; $\varphi = 0–360°$, $ss = 3°$ and $st = 3$ s, and the 204 pole figure at $2\theta = 36.716°$; $\chi = 6–42°$, $ss = 3°$; $\varphi = 0–360°$, $ss = 3°$ and $st = 3$ s.

Received: November 30, 2005
Final version: March 20, 2006
Published online: August 8, 2006

[1] J. Trull, R. Vilaseca, J. Martorell, R. Corbalan, *Opt. Lett.* **1995**, *20*, 1746.
[2] P. P. Markowicz, H. Tiryaki, H. Pudavar, P. N. Prasad, N. Lepeshkin, R. W. Boyd, *Phys. Rev. Lett.* **2004**, *92*, 083 903.
[3] J. Torres, M. Le Vassoi d'Yerville, D. Coquillat, E. Centeno, J. P. Albert, *Phys. Rev. B: Condens. Matter Mater. Phys.* **2005**, *71*, 195 326.
[4] J. Martorell, R. Vilaseca, R. Corbalan, *Appl. Phys. Lett.* **1997**, *70*, 702.
[5] M. Centini, C. Sibilia, M. Scalora, G. D'Aguanno, M. Bertolotti, M. J. Bloemer, C. M. Bowden, I. Nefedov, *Phys. Rev. E: Stat., Nonlinear, Soft Matter Phys.* **1999**, *60*, 4891.
[6] J. Martorell, R. Vilaseca, R. Corbalan, *Phys. Rev. A: At., Mol., Opt. Phys.* **1997**, *55*, 4520.
[7] J. Martorell, *Appl. Phys. Lett.* **2005**, *86*, 241 113.
[8] S. Noda, M. Imada, M. Okano, S. Ogawa, M. Mochizuki, A. Chutinan, *IEEE J. Quantum Electron.* **2002**, *38*, 726.
[9] M. François, J. Danglot, B. Grimbert, P. Mounaix, M. Muller, O. Vanbésien, D. Lippens, *Microelectron. Eng.* **2002**, *61–62*, 537.
[10] A. M. Malvezzi, F. Cattaneo, G. Vecchi, M. Falasconi, G. Guizzetti, L. C. Andreani, F. Romanato, L. Businaro, E. Di Fabrizio, A. Passaseo M. Di Vittorio, *J. Opt. Soc. Am. B* **2002**, *19*, 2122.
[11] G. Vecchi, J. Torres, D. Coquillat, M. Le Vassor d'Yerville, A. M. Malvezzi, *Appl. Phys. Lett.* **2004**, *84*, 1245.
[12] A. Birner, R. B. Wehrspohn, U. M. Gösele, K. Busch, *Adv. Mater.* **2001**, *13*, 377.
[13] K. Avary, J. P. Reithmeier, F. Klopf, T. Happ, M. Kamp, A. Forchel, *Microelectron. Eng.* **2002**, *61–62*, 875.
[14] C. Monat, C. Seassal, X. Letartre, P. Regreny, P. Rojo-Romeo, P. Viktorovitch, M. Le Vassor d'Yerville, D. Cassagne, J. P. Albert, E. Jalaguier, S. Pocas, B. Aspar, *Appl. Phys. Lett.* **2002**, *81*, 5102.
[15] F. Lacour, N. Courjal, M.-P. Bernal, A. Sabac, C. Bainier, M. Spajer, *Opt. Mater.* **2005**, *27*, 4121.
[16] M. N. Satyanarayan, A. Deepthy, H. L. Bhat, *Crit. Rev. Solid State Mater. Sci.* **1999**, *24*, 103.
[17] L.-H. Peng, C.-C. Hsu, J. Ng, A. H. Kung, *Appl. Phys. Lett.* **2005**, *84*, 3250.
[18] C. Canalias, V. Pasiskevicius, M. Fokine, F. Laurell, *Appl. Phys. Lett.* **2005**, *86*, 181 105.
[19] J. Schilling, A. Birner, F. Müller, R. B. Wehrspohn, R. Hillebrand, U. Gösele, K. Busch, S. John, S. W. Leonard, H. M. van Driel, *Opt. Mater.* **2001**, *17*, 7.
[20] V. Lehmann, H. Föll, *J. Electrochem. Soc.* **1990**, *137*, 653.
[21] P. A. Thomas, A. M. Glazer, B. E. Watts, *Acta Crystallogr., Sect. B: Struct. Sci.* **1990**, *46*, 333.
[22] M. Galli, M. Agio, L. C. Andreani, M. Belotti, G. Guizzetti, F. Marabelli, M. Patrini, P. Bettotti, L. Dal Negro, Z. Gaburro, L. Pavesi, A. Lui, P. Bellutti, *Phys. Rev. B: Condens. Matter Mater. Phys.* **2002**, *65*, 113 111.
[23] "Translight" software package by A. L. Reynolds, University of Glasgow, 2000.
[24] K. Sakoda, *Optical Properties of Photonic Crystals*, Springer, Berlin **2001**, p. 111.
[25] V. Lehmann, *J. Electrochem. Soc.* **1993**, *140*, 2836.
[26] J. C. Jacco, G. M. Loiacono, M. Jaso, G. Mizell, B. Greenberg, *J. Cryst. Growth* **1984**, *70*, 484.
[27] R. A. Laudise, R. J. Cava, A. J. Caporaso, *J. Cryst. Growth* **1986**, *74*, 275.
[28] R. Solé, V. Nikolov, A. Vilalta, J. J. Carvajal, J. Massons, J. Gavaldà, M. Aguiló, F. Díaz, *J. Mater. Res.* **2002**, *17*, 563.

